FISEVIER

Contents lists available at ScienceDirect

Journal of Magnetism and Magnetic Materials

journal homepage: www.elsevier.com/locate/jmmm



Pressure modulated spin-gapless semiconductivity in FeCrTiAl

Pavel V. Lukashev a,*, Stephen McFadden , Paul M. Shand , Parashu Kharel b

ARTICLE INFO

Keywords: Spin-gapless semiconductors Half-metals Heusler alloys Spintronics

ABSTRACT

Spin-gapless semiconductors (SGS) represent a new type of compounds with potential applications in novel spintronic devices. Here, we performed a comprehensive computational and theoretical study of FeCrTiAl, a quaternary Heusler compound that was recently predicted to exhibit nearly SGS properties. Our calculations indicate that this material undergoes several band structure transitions from essentially semimetallic phase at smaller lattice constants to nearly type-II SGS at the ground state, then to nearly type-III SGS and further to nearly type-I SGS, as the lattice parameter is increased. Another interesting feature of FeCrTiAl is that its spin polarization changes sign from negative to positive as the volume of the cell increases. At the largest considered lattice parameters, this compound exhibits nearly 100% spin polarization. The mechanical expansion discussed in this text may be achieved, in principle, either by applying an epitaxial strain in thin-film geometry, or by chemical substitution, for example with non-magnetic element of larger atomic radius. We hope that the presented results may provide guidance for further research on mechanical strain induced manipulation of electronic and magnetic properties of spin-gapless semiconductors.

1. Introduction

Spin-gapless semiconductors represent a relatively new class of materials, intended for potential device applications in spin-based electronics (spintronics). The existence of these materials was theoretically predicted by X. L. Wang in 2008 [1]. The electronic structure of SGS somewhat resembles a more familiar class of materials, known as half-metals (HM). Both are expected to provide 100% spin-polarization in ideal circumstances, such as no impurities and other structural defects, and no detrimental contribution from surface states in thin-film geometry [2,3]. In practice, however, these effects can rarely be avoided, so the actual measured values of spin-polarization reported in experimental literature are usually less than 100% [4]. Still, these materials are considered among the best candidates for generating highly spin-polarized current, which is the cornerstone of spintronics.

Although somewhat similar, the electronic structure of HM and SGS materials has one distinct difference, which may be summarized as follows. Half-metallic compounds are conductors for one spin, and insulators for the opposite spin. On the other hand, spin-gapless semiconductors are insulators for one spin, and gapless semiconductors for the opposite spin. In addition, the gapless character of SGS materials may be exhibited in four different ways, as proposed initially by X. L.

Wang [1]. In the first case, one of the spin channels has energy gap, while the other spin channel is gapless (type-I). In the second case, both spin channels have energy gap, but the gapless nature of the electronic structure is produced by the valence band maximum (VBM) of majority-spin electrons and conduction band minimum (CBM) of minority-spin electrons touching each other at the Fermi level (type-II). In the third case, valence band maximum is produced by one spin channel, while conduction band minimum comes from both spin channels (type-III). Finally, another possibility is when CBM is produced by one spin channel, while VBM originates from both spin channels (type-IV). More details (with examples) of these four types of SGS band structures may be found in recent literature [5,6].

Although the electronic structure of both half-metallic and spingapless semiconducting materials is usually very sensitive to various physical mechanisms, such as mechanical strain, reduced geometry, and atomic disorder [7–15], spin-gapless semiconductors are somewhat more sensitive, since the gapless nature of the band structure can easily be destroyed by the mentioned physical mechanisms [3]. Therefore, it is interesting to analyze how some of these mechanisms modify the properties of SGS compounds, as this information may be useful for practical implementations, where ideal circumstances (such as disorderfree crystal structures and equilibrium lattice parameters) may be

E-mail address: pavel.lukashev@uni.edu (P.V. Lukashev).

^a Department of Physics, University of Northern Iowa, Cedar Falls, IA 50614, USA

^b Department of Physics, South Dakota State University, Brookings, SD 57007, USA

^{*} Corresponding author.

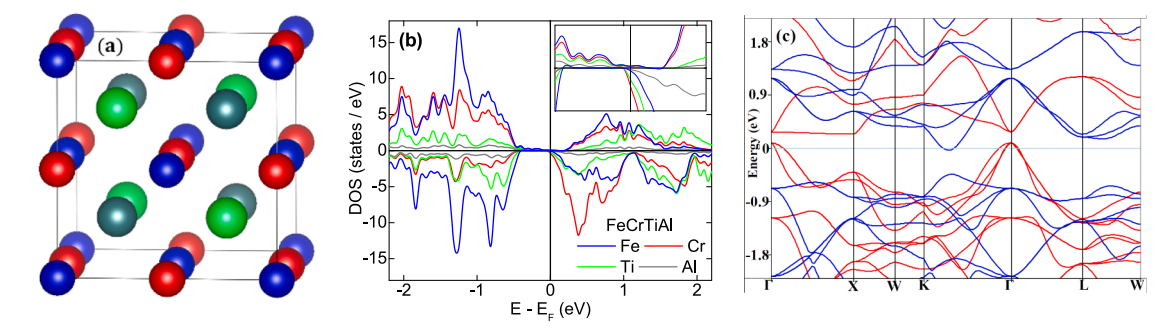


Fig. 1. (a) Regular cubic Heusler crystal structure of FeCrTiAl. Atoms are colored as follows: Fe – blue, Cr – red, Ti – green, Al – gray. (b) Calculated element- and spin-resolved density of states (DOS) of FeCrTiAl at equilibrium. Atomic contributions are colored as indicated in the figure, consistent with the coloring scheme used in Fig. 1 (a). Positive and negative DOS indicate majority and minority spin contributions, correspondingly. Vertical line indicates position of Fermi level. The inset shows DOS around Fermi energy. (c) Calculated electronic band structure of FeCrTiAl at equilibrium, along symmetry points shown in the figure. Zero energy corresponds to Fermi level. Red and blue lines show majority and minority spin bands, correspondingly. (For interpretation of the references to colour in this figure legend, the reader is referred to the web version of this article.)

uncommon [3].

Half-metallic Heusler alloys attracted particular attention of spintronic community, as they often exhibit high Curie temperature, [16] much higher than the room temperature [17-23]. In addition, they may be relatively easy to synthesize experimentally and study theoretically, as they usually exhibit a regular cubic structure. Here, we present a comprehensive study of FeCrTiAl, a quaternary Heusler compound that has been recently reported to exhibit SGS properties [5,6]. Our results indicate that the electronic structure of this material undergoes several transitions under external mechanical strain. In particular, at smaller lattice constants, this material may be characterized as semimetallic. As the lattice constant increases, it undergoes a transition to quasi-type-II SGS, at around equilibrium. As the lattice constant increases further, a quasi-type-II SGS electronic structure is modified into quasi-type-III SGS. Further increase of the lattice constant (to the region which may be difficult to realize in practice, except maybe in thin-film geometry), a quasi-type-III SGS electronic structure is modified into a quasi-type-I SGS. Our hope is that these results may be useful for further research on strain induced manipulation of electronic and magnetic properties of spin-gapless semiconductors.

The article is organized as follows. The computational details are summarized in the next section. It follows by the main results and discussion. This section consists of two parts: ground state properties, and the effect of hydrostatic pressure. The paper is summarized with concluding remarks, acknowledgments, and references to relevant literature.

2. Computational methods

Results reported in this work are obtained using the Vienna *ab initio* simulation package (VASP) [24]. The calculations are performed within the projector augmented-wave method (PAW)[25] and generalized-gradient approximation (GGA) [26]. The Hubbard U correction is not included in our calculations because the considered material is metallic, except maybe at the very large lattice parameters. The correlation effects are more important in magnetic insulators, while metallic systems are typically adequately described within regular GGA. We used the integration method by Methfessel and Paxton [27] with a cut-off energy of 500 eV. The Brillouin-zone integration is performed with the *k*-point mesh of $12 \times 12 \times 12$ for all electronic structure calculations. The energy convergence condition is set to 10^{-3} meV. The band structures are obtained and visualized using the MedeA® software environment [28].

All calculations performed in this work are done using the Advanced Cyberinfrastructure Coordination Ecosystem: Services & Support (ACCESS) (formerly known as Extreme Science and Engineering Discovery Environment (XSEDE)) resources located at the Pittsburgh Supercomputing Center (PSC) [29], and with the resources of the Center for Functional Nanomaterials (CFN) at Brookhaven National Laboratory (BNL).

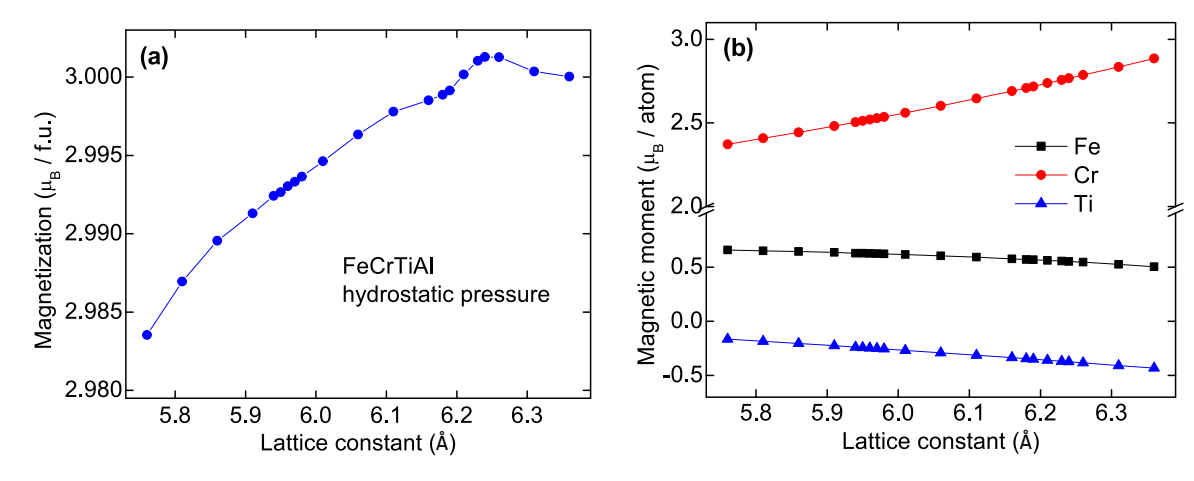


Fig. 2. (a) Calculated magnetization (a), and magnetic moment per atom (b) of FeCrTiAl under uniform (hydrostatic) pressure. Atomic contributions are indicated in the figure.

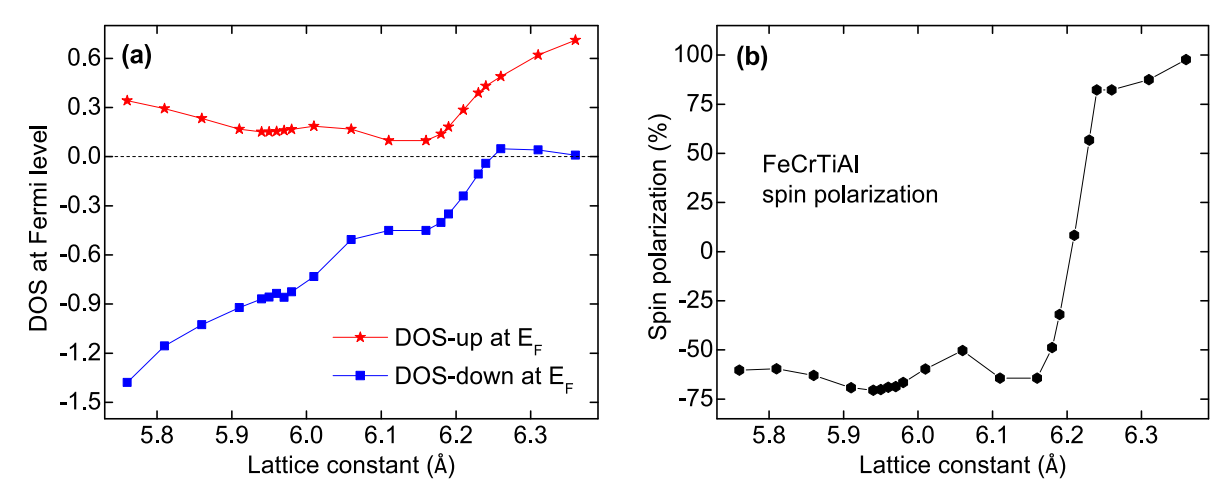


Fig. 3. (a) Calculated total DOS at Fermi level (a), and spin polarization (b) of FeCrTiAl under uniform (hydrostatic) pressure. Positive / negative DOS in (a) correspond to majority / minority spin contribution, correspondingly. Small positive DOS of minority spin at larger lattice constants is probably a computational artifact

3. Results and discussion

3.1. Ground state properties of FeCrTiAl

FeCrTiAl belongs to a regular cubic Heusler structure (space group F-43 m), with the following Wyckoff positions: Fe (0,0,0), Cr (1/2,1/2,1/2), Ti (3/4,3/4), Al (1/4,1/4,1/4). The unit cell of this structure is shown in the Fig. 1 (a). The calculated equilibrium lattice constant is 5.961 Å, in agreement with recent reports by Dhakal, et al. [5], and Gao, et al. [6]. The magnetic moments of FeCrTiAl align ferrimagnetically, in particular a relatively small moment of Ti (-0.246 μ_B) is anti-aligned with the moments of Fe (0.626 μ_B) and Cr (2.520 μ_B), Al being non-magnetic. The calculated magnetization is 2.993 μ_B / f.u. A small deviation between the total calculated magnetization and the sum of individual atomic moments results from the local magnetic moments being calculated in atomic spheres which do not precisely fill the entire volume of the unit cell. A nearly integer magnetization value may indicate that this material is almost perfectly spin-polarized, which is confirmed by the electronic structure analysis presented below.

Fig. 1 shows the calculated density of states (DOS) (b) and electronic $\,$

band structure (c) of FeCrTiAl at the equilibrium lattice constant. As these figures illustrate, FeCrTiAl is probably best described as a semimetal in its ground state. Moreover, it appears that a potential transition to spin-gapless semiconducting state can not be induced by a rigid shift of Fermi level, e.g. by external pressure, or atomic substitution. In particular, such hypothetical shift of Fermi level towards the filled states could potentially results in half-metallic (but not SGS) transition. At the same time, if the Fermi level is shifted towards the unoccupied states, this material may, at least in principle, undergo a transition to halfmetallic state (but again, not SGS) with very small energy gap (~0.1 eV) in the majority spin channel. The only hypothetically possible scenario to induce SGS transition in FeCrTiAl appears to be a modification of exchange splitting around Fermi level. In particular, if Fermi level is rigidly shifted towards the lower energy minority spin states by ~ 0.2 eV, while simultaneously being shifted by the same amount towards the higher energy majority spin states, this could, at least in principle, results in a transition to a perfect spin-gapless semiconducting structure. With this in mind, in the next sub-section we analyze the effect of mechanical strain on electronic structure of FeCrTiAl.

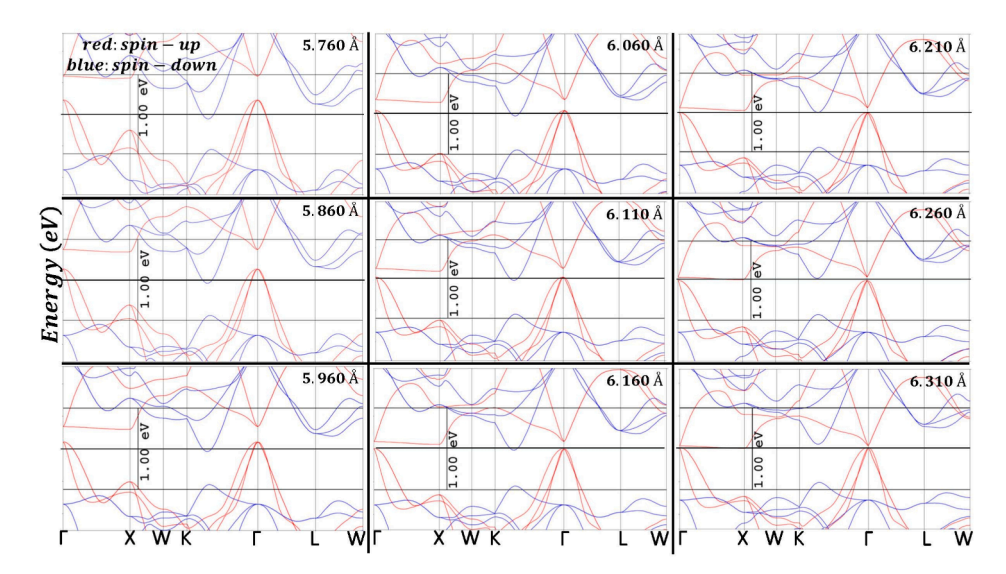


Fig. 4. (a) Calculated electronic band structure of FeCrTiAl under uniform (hydrostatic) pressure. Lattice parameters at which the band structure is calculated are shown in the figure. The solid horizontal line in the center of each plot indicates the position of Fermi level. The energy range is visualized by a vertical 1.00 eV interval on each plot.

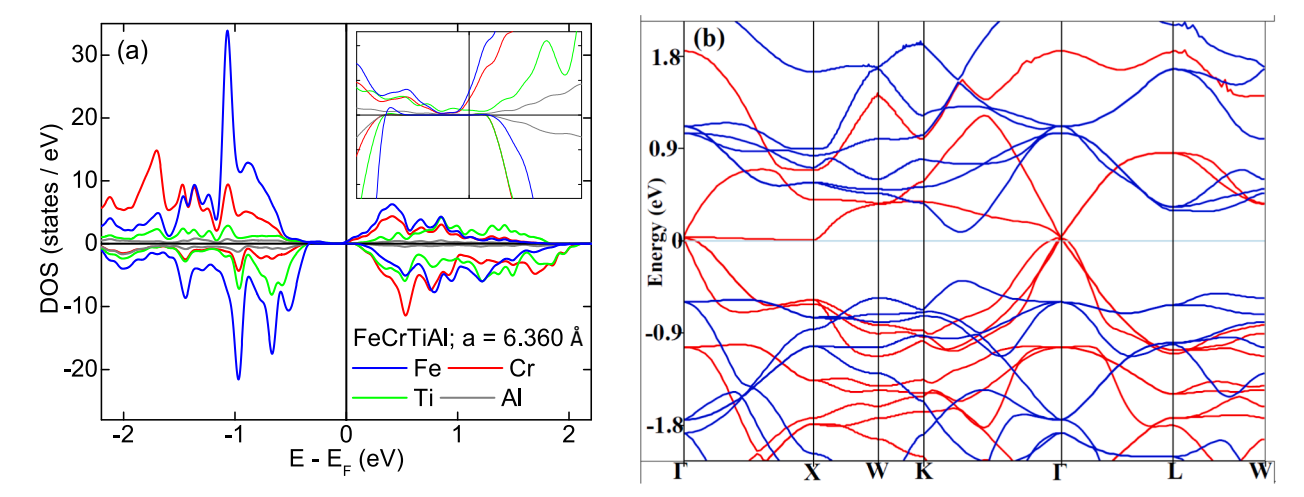


Fig. 5. (a) Calculated element- and spin- resolved density of states (DOS) of FeCrTiAl at the lattice constant, $a=6.360\,\text{Å}$. Atomic contributions are colored as indicated in the figure. Positive and negative DOS indicate majority and minority spin contributions, correspondingly. Vertical line indicates position of Fermi level. The inset shows DOS around Fermi energy. (b) Calculated electronic band structure of FeCrTiAl at the lattice constant, $a=6.360\,\text{Å}$, along symmetry points shown in the figure. Zero energy corresponds to Fermi level. Red and blue lines show majority and minority spin bands, correspondingly. (For interpretation of the references to colour in this figure legend, the reader is referred to the web version of this article.)

3.2. Strain modulated properties of FeCrTiAl

Fig. 2 shows calculated magnetization (total magnetic moment / f.u.) (a), and magnetic moments per atom (b) of FeCrTiAl under uniform (hydrostatic) pressure. One can see that increasing lattice constant results in increase of magnetization, until it somewhat saturates at around $3.000 \mu_B$ / f.u. The integer magnetization value may serve as an indication of transition to 100% spin-polarized state, which will be discussed in more detail below. Fig. 2 (b) shows dependence of individual magnetic moments of FeCrTiAl on uniform pressure. First, this figure confirms the ferrimagnetic nature of this compound. In particular, the magnetic moment of Ti is anti-aligned with the magnetic moments of Fe and Cr. Increasing the lattice constant results in increase (by the absolute value) of Cr and Ti magnetic moments. At the same time, the magnetic moment of Fe is decreasing at larger lattice constants. Thus, the overall contribution of Fe and Ti is to reduce the magnetization of FeCrTiAl as the lattice parameter is increased. At the same time, the magnetic moment of Cr increases rather significantly as the volume of the cell increases, and as a result the overall magnetization of the cell goes up, albeit by a relatively small amount.

Fig. 3 shows calculated spin-resolved total density of states at Fermi level (a), and calculated spin-polarization of FeCrTiAl, as a function of lattice parameter. Here, the spin polarization is calculated as $P=\frac{N\uparrow(E_F)-N\downarrow(E_F)}{N\uparrow(E_F)+N\downarrow(E_F)}$, where $N_{\uparrow\downarrow}(E_F)$ is the spin-dependent DOS at the Fermi level, E_F [30]. A small positive DOS of minority spin at larger lattice constants is probably a computational artifact, as mentioned in the figure caption. As shown in Fig. 3 (b), at smaller lattice constants, FeCrTiAl has a negative spin polarization, corresponding to larger spin-down DOS than spin-up DOS at Fermi level. This can be also seen in the inset of Fig. 1 (b), which shows the DOS distribution around Fermi energy. At the same time, at larger lattice constants, the spin polarization changes sign and finally reaches almost 100% (98%, to be precise) at the largest considered lattice parameter. This confirms our earlier argument that nearly integer magnetization values at the large lattice constant may be an indication of nearly 100% spin polarized state.

Fig. 4 shows evolution of the calculated electronic band structure of FeCrTiAl under hydrostatic pressure. First, we notice that at the smallest considered lattice constants this material is essentially semimetallic. As the lattice constant is increased, at around equilibrium the electronic structure of this materials starts resembling a quasi-type-II SGS behavior. Ideal type-II spin-gapless semiconductor has energy gaps in both spin-up and spin-down states. The gapless nature of the band

structure is produced by the valence band maximum of the spin-up (see red lines in Fig. 4) and the conduction band minimum of spin-down (see blue lines in Fig. 4) states touching each other at the Fermi energy (at different symmetry points, thus resulting in indirect zero band gap). At the equilibrium value of the lattice constant of ~ 5.96 Å, this feature comes close to being implemented. The small deviation from the perfect type-II SGS follows from a small crossover of spin-up VBM and spindown CBM at the Fermi level. These results are consistent with a recent report by Dhakal, et al. [5]. The crossover of spin-up VBM and spin-down CBM at the Fermi level increases at smaller lattice constants, thus producing a semimetallic behavior. At the same time, as the lattice constant of this material is increased beyond equilibrium, a transition to nearly perfect type-III SGS behavior is seen. Indeed, at around 6.20 Å, almost perfect gapless character is produced by valence band maximum of spin-up states (red line) and conduction band minimum of both spinup (red line) and spin-down (blue line) states. As the lattice constant is increased further, the crossover of spin-up VBM and spin-down CBM at the Fermi level decreases and then disappears altogether. In particular, at around a = 6.31 Å, the band structure of FeCrTiAl very closely resembles type-I SGS features, with a clear band gap of spin-down states (blue line), and nearly gapless character of spin-up bands (red line). At that point, this compound becomes nearly 100% spin polarized.

To illustrate these features more clearly, we plot both DOS and band structure of FeCrTiAl at $a=6.360\,\text{\AA}$, see Fig. 5. This lattice constant is likely too large to be implemented in practice, except maybe in thin-film geometry, where larger values of mechanical strain are feasible (atomic substitution may also, in principle, result in larger equilibrium lattice parameter). Thus, Fig. 5 mostly serves as an illustration of (somewhat hypothetical) electronic structure of FeCrTiAl in quasi-type-I SGS phase. We use the term "quasi" here, since there is still a small crossing of Fermi level by spin-up states at the Γ -point (see Fig. 5 (b)). If this crossing was absent, we would have a perfect type-I SGS material, with a band gap in one spin channel, and a gapless electronic structure in the opposite spin.

4. Conclusion

Here, we performed a comprehensive computational and theoretical study of FeCrTiAl, a quaternary Heusler compound that was predicted recently to exhibit nearly spin-gapless semiconducting behavior. Our results indicate that this material is semimetallic at smaller lattice constants. As the cell volume is increased, FeCrTiAl undergoes a transition to what could be classified as quasi-type-II SGS phase, at around

equilibrium lattice constant. Further increase of the lattice constant results in a quasi-type-II SGS to quasi-type-III SGS, and then quasi-type-III SGS to nearly perfect type-I SGS transitions. In addition, the spin polarization of this material undergoes a change in sign, from negative to positive, as the lattice constant is increased. In principle, a negative pressure (mechanical expansion) may be achieved either by applying an epitaxial strain in thin-film geometry, or by chemical substitution, e.g. with non-magnetic element of larger atomic radius. We hope that the presented results, in particular several electronic structure transitions of this compound under mechanical pressure may be useful for researchers working on spin-gapless semiconductors, and may spark further work by experimental groups on this and similar alloys.

CRediT authorship contribution statement

Pavel V. Lukashev: Conceptualization, Formal analysis, Funding acquisition, Investigation, Project administration, Supervision, Writing – original draft, Writing – review & editing. **Stephen McFadden:** Investigation, Validation, Visualization. **Paul M. Shand:** Conceptualization, Formal analysis, Funding acquisition, Investigation, Writing – review & editing. **Parashu Kharel:** Conceptualization, Formal analysis, Funding acquisition, Investigation, Writing – review & editing.

Declaration of Competing Interest

The authors declare that they have no known competing financial interests or personal relationships that could have appeared to influence the work reported in this paper.

Data availability

Data will be made available on request.

Acknowledgments

This research is supported by the National Science Foundation (NSF) under Grant Numbers 2003828 and 2003856 via DMR and EPSCoR. This work used the Advanced Cyberinfrastructure Coordination Ecosystem: Services & Support (ACCESS) (formerly known as Extreme Science and Engineering Discovery Environment (XSEDE)), which is supported by National Science Foundation grant number ACI-1548562. This work used the XSEDE Regular Memory (Bridges 2) and Storage (Bridges Ocean) at the Pittsburgh Supercomputing Center (PSC) through allocation TG-DMR180059, and the resources of the Center for Functional Nanomaterials, which is a U.S. DOE Office of Science Facility, and the Scientific Data and Computing Center, a component of the

Computational Science Initiative, at Brookhaven National Laboratory (BNL) under Contract No. DE-SC0012704.

References

- [1] X.L. Wang, Phys. Rev. Lett. 100 (2008), 156404.
- [2] E. O'Leary, B. Dahal, P. Kharel, P. Lukashev, J. Magn. Magn. Mater. 514 (2020), 167188.
- [3] P. Lukashev, P. Kharel, S. Gilbert, B. Staten, N. Hurley, R. Fuglsby, Y. Huh, S. Valloppilly, W. Zhang, K. Yang, R. Skomski, D.J. Sellmyer, Appl. Phys. Lett. 108 (2016), 141901.
- [4] M. Jourdan, J. Minár, J. Braun, A. Kronenberg, S. Chadov, B. Balke, A. Gloskovskii, M. Kolbe, H.J. Elmers, G. Schönhense, H. Ebert, C. Felser, M. Kläui, Nat. Commun. 5 (2014) 3974.
- [5] R. Dhakal, S. Nepal, I. Galanakis, R.P. Adhikari, G.C. Kaphle, J. Alloy. Compd. 882 (2021), 160500.
- [6] Q. Gao, I. Opahle, H. Zhang, Phys. Rev. Materials 3 (2019), 024410.
- [7] W. Zhu, B. Sinkovic, E. Vescovo, C. Tanaka, J.S. Moodera, Phys. Rev. B 64 (2001) R060403.
- [8] A.N. Caruso, C.N. Borca, D. Ristoiu, J.P. Nozieres, P.A. Dowben, Surf. Sci. 525 (2003) L109.
- [9] D. Ristoiu, J.P. Nozières, C.N. Borca, B. Borca, P.A. Dowben, Appl. Phys. Lett. 76 (2000) 2349.
- [10] I. Galanakis, J. Phys. Condens. Matter 14 (2002) 6329.
- [11] M. Ležaic, I. Galanakis, G. Bihlmayer, S. Blügel, J. Phys. Condens. Matter 17 (2005) 3121.
- [12] P. Kharel, W. Zhang, R. Skomski, S. Valloppilly, Y. Huh, R. Fuglsby, S. Gilbert, D. J. Sellmyer, Phys. D: Appl. Phys. 48 (2015), 245002.
- [13] J. Herran, R. Dalal, P. Gray, P. Kharel, P. Lukashev, J. Appl. Phys. 122 (2017), 153904.
- [14] I. Tutic, J. Herran, B. Staten, P. Gray, T. Paudel, A. Sokolov, E. Tsymbal, P. Lukashev, J. Phys. Condens. Matter 29 (2017), 075801.
- [15] L. Stuelke, L. Margaryan, P. Kharel, P. Shand, P. Lukashev, J. Magn. Magn. Mater. 553 (2022), 169267.
- [16] A. Nelson, P. Kharel, Y. Huh, R. Fuglsby, J. Guenther, W. Zhang, B. Staten, P. Lukashev, S. Valloppilly, D.J. Sellmyer, J. Appl. Phys. 117 (2015), 153906.
- [17] R.A. de Groot, F.M. Mueller, P.G. van Engen, K.H.J. Buschow, Phys. Rev. Lett. 50 (1983) 2024.
- [18] I. Galanakis, P.H. Dederichs, N. Papanikolaou, Phys. Rev. B 66 (2002), 174429.
- [19] E. Şaşıoğlu, L.M. Sandratskii, P. Bruno, Phys. Rev. B 72 (2005), 184415.
- [20] B. Balke, G.H. Fecher, J. Winterlik, C. Felser, Appl. Phys. Lett. 90 (2007), 152504.
- [21] H. Kurt, K. Rode, M. Venkatesan, P. Stamenov, J.M.D. Coey, Phys. Status Solidi B 248 (2011) 2338.
- [22] J. Winterlik, S. Chadov, A. Gupta, V. Alijani, T. Gasi, K. Filsinger, B. Balke, G. H. Fecher, C.A. Jenkins, F. Casper, J. Kübler, G. Liu, L. Gao, S.S.P. Parkin, C. Felser, Adv. Mater. 24 (2012) 6283.
- [23] I. Galanakis, in Heusler Alloys, Springer Series in Materials Science 222, C. Felser and A. Hirohata (eds.), Springer International Publishing Switzerland 2016.
- [24] G. Kresse, D. Joubert, Phys. Rev. B 59 (1999) 1758.
- [25] P. Blöchl, Phys. Rev. B 50 (1994) 17953.
- [26] J.P. Perdew, K. Burke, M. Ernzerhof, Phys. Rev. Lett. 77 (1996) 3865.
- [27] M. Methfessel, A.T. Paxton, Phys. Rev. B 40 (1989) 3616.
- [28] MedeA-2.22, Materials Design, Inc., San Diego, CA, USA, 2017.
- [29] J. Towns, T. Cockerill, M. Dahan, I. Foster, K. Gaither, A. Grimshaw, V. Hazlewood, S. Lathrop, D. Lifka, G.D. Peterson, R. Roskies, J.R. Scott, N. Wilkins-Diehr, XSEDE: Accelerating Scientific Discovery, Comput. Sci. Eng. 16 (5) (2014) 62–74.
- [30] J.P. Velev, P.A. Dowben, E.Y. Tsymbal, S.J. Jenkins, A.N. Caruso, Surf. Sci. Rep. 63 (2008) 400.